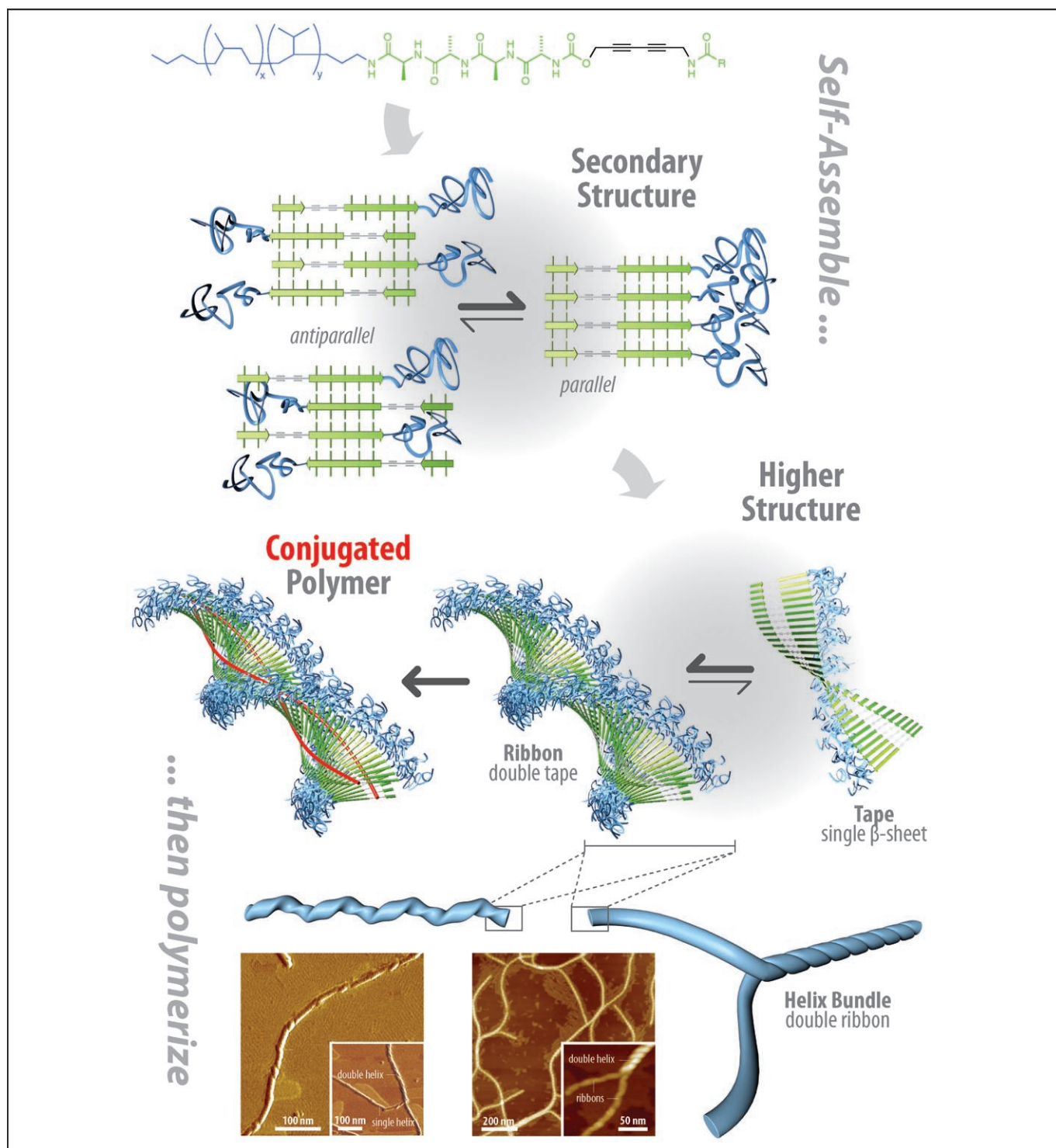


# A General Concept for the Preparation of Hierarchically Structured $\pi$ -Conjugated Polymers

Holger Frauenrath\* and Eike Jahnke<sup>[a]</sup>



**Abstract:** Typical biopolymers exhibit structures and order on different length scales. By contrast, the number of synthetic polymers with a similar degree of hierarchical structure formation is still limited. Starting from recent investigations on the structures of amyloid proteins as well as research activities toward nanoscopic scaffolds from synthetic oligopeptides and their polymer conjugates, a general strategy toward hierarchically structured  $\pi$ -conjugated polymers can be developed. The approach relies on the supramolecular self-assembly of diacetylene macromonomers based on  $\beta$ -sheet forming oligopeptides equipped with hydrophobic polymer segments. Polymerization of these macromonomers proceeds under retention of the previously assembled hierarchical structure and yields  $\pi$ -conjugated polymers with multi-stranded, multiple-helical quaternary structures.

**Keywords:** biopolymers • nanostructures • peptides • polymerization • self-assembly

## Introduction

Biomaterials such as silk, collagen, or wood often exhibit extraordinary properties, which is even more remarkable as they are produced under mild, physiological conditions. One of the origins of these features is the fact that biopolymers typically exhibit structure and order on different length scales. In proteins, for example, the amino acid sequence (primary structure) predetermines different chain segments to attain well-defined conformations like, for instance,  $\alpha$ -helices or  $\beta$ -sheets (secondary structure). These are then folded into a specific spatial arrangement (tertiary structure) that determines the overall topographic shape of the macromolecules in solution. Finally, several of these folded macromolecules may serve as subunits that self-assemble into the active protein complex or structure protein (quaternary structure). Biological systems often achieve this kind of hierarchical structure formation utilizing a combined “bottom-up” and “top-down” approach. Thus, the information to adopt a certain higher structure is programmed on the molecular level. At the same time, the macromolecules are carefully guided to find the desired structure among the manifold of energetically similar possibilities, for instance, by using template molecules (e.g., chaperone proteins) or by means of sophisticated processing procedures (e.g., the spinning of a spider silk thread).

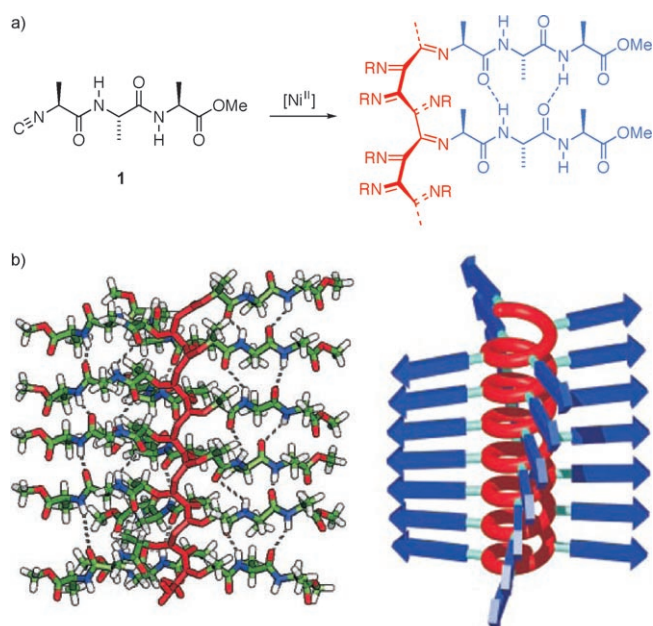
Accordingly, the preparation of hierarchically structured synthetic polymers has been recognized as an important field of research.<sup>[1]</sup> However, while polymer chemists have been striving to understand the basic principles of hierarchical structure formation in biopolymers over the past three decades and huge progress has been made on the field of synthetic polymer chemistry in general, the tools at hand to exert a control of polymer structure comparable to biological systems are still limited in scope.<sup>[1d]</sup> Recent successful attempts to prepare hierarchically structured polymer materials were based on strategies which aimed to combine modern organic and polymer chemistry,<sup>[1e]</sup> as well as materials science and supramolecular chemistry.<sup>[1f]</sup> Supramolecular self-assembly has already been extensively investigated as a tool to create hierarchically structured, optoelectronically active materials from monodisperse,  $\pi$ -conjugated oligomers.<sup>[2]</sup> The “supramolecular approach” attempts to alleviate the shortcomings of common processing procedures such as chemical vapor deposition by providing a pathway toward highly ordered, nanostructured arrays of  $\pi$ -conjugated oligomers from solution.

This Concept paper aims to demonstrate how the supramolecular approach can be extended toward the preparation of hierarchically structured,  $\pi$ -conjugated polymers. With the help of selected examples, we wish to develop a general strategy towards the preparation of such polymers based on the supramolecular self-assembly of oligopeptide–polymer conjugates. Thus, a concise overview of the structures of amyloid proteins as well as the supramolecular self-assembly of short oligopeptides and their polymer conjugates will serve to explain why and how exactly the latter can be designed and utilized as supramolecular scaffolds for this specific purpose. Finally, we will summarize and explain how these scaffolds can be used in the preparation of well-defined, soluble  $\pi$ -conjugated polymers with predictable multi-stranded, multiple-helical quaternary structures.

## Hierarchically Structured Polymers via the Foldamer Approach

In the realm of conventional synthetic polymers, the most successful examples of hierarchically structured polymers resulted from transferring the “foldamer” concept<sup>[3]</sup> to the world of high molecular weight polymer materials. In one incarnation of this approach, the polymers comprise interactions between “sticky sites” in the side chains of non-adjacent repeating units. These serve to induce the formation of stable folded conformations due to cooperative intrachain supramolecular interactions and, thus, mimic the folding mechanism observed in biopolymers. The preparation of oligopeptide-substituted poly(isocyanide)s **1** and their block copolymers reported by the groups of Nolte and Cornelissen represents a particularly beautiful implementation of that concept (Figure 1).<sup>[4]</sup> The number of hierarchically struc-

[a] Dr. H. Frauenrath, E. Jahnke  
ETH Zürich, Department of Materials  
Wolfgang-Pauli-Strasse 10, HCI H515, 8093 Zürich (Schweiz)  
Fax: (+41)44-633-1390  
E-mail: frauenrath@mat.ethz.ch

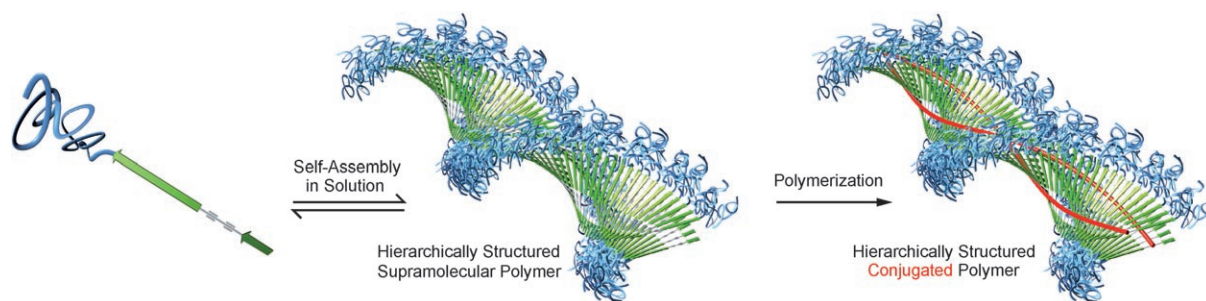


tured  $\pi$ -conjugated polymers, on the other hand, is very limited to date, mainly due to the demanding synthetic requirements. Notably, Masuda and co-workers have published a large body of investigations on poly(acetylene)s with hydrogen-bonded side chains which may be regarded as foldamers.<sup>[5]</sup> The authors interpreted the increased rigidity upon the incorporation of homochiral side chains, the large optical rotations of the polymers, and the strong CD effect of the main chain chromophore in terms of stable folded conformations due to cooperative intramolecular hydrogen bonding.

### "Self-Assemble into a Hierarchical Structure, then Polymerize"—A Complementary Approach

In the preceding examples, the hierarchically structured synthetic polymers have been prepared using a general approach that can be described as "polymerize, then fold into a hierarchical structure". Alternatively, one may envisage to reverse the order of the required steps and develop a complementary strategy which may be paraphrased as "self-assemble into a hierarchical structure, then polymerize" (Figure 2).<sup>[6]</sup> Thus, appropriately functionalized macromonomers are supposed to first self-assemble into uniform supramolecular polymers with a defined, finite number of strands, as opposed to micellar or vesicular one-dimensional aggregates. These supramolecular polymers should, at the same time, show a propensity to hierarchical structure formation in solution. They are then to be converted into functional, possibly multi-stranded polymers under retention or, at least, controlled conversion of their previously assembled hierarchical structure.

This general strategy toward hierarchically structured, conjugated polymers would, hence, combine the supramolecular preorganization of monomers prior to polymerization<sup>[6]</sup> with covalent capture as a versatile concept for the fixation of supramolecular materials.<sup>[7]</sup> Furthermore, it may leverage "structural self-healing" as one of the crucial advantages of the supramolecular self-assembly of oligomers to the preparation of high molecular weight  $\pi$ -conjugated polymers. It is worth noting that the "foldamer approach" is limited by the inherently poor control over the polymer primary structure that can be achieved even with modern polymerization methods, for instance, in terms of regioselectivity and stereospecificity of monomer incorporation. This limitation is detrimental to the efficient and defect-free folding into the final conformation. In case of a low degree of tacticity, for example, any stereochemical defect will irreversibly be incorporated into the polymer, and the subsequent folding may fail or produce defective structures. By contrast, dynamic self-assembly prior to fixation by polymerization may allow defects to be corrected and the hierarchical structure to be controlled or fine-tuned by changing the temperature, the solvent or other external parameters.



On the other hand, most covalent capture processes will inevitably result in structural reorganisations which may even destroy the self-assembled hierarchical structures. Therefore, a number of requirements will have to be fulfilled in order for the proposed complementary strategy to be successfully applied:

- Most importantly, a reliable supramolecular synthon<sup>[8]</sup> is needed that will give rise to the formation of uniform supramolecular polymers with a defined, finite number of polymer strands.
- These supramolecular polymers must have the propensity to show predictable or, at least, rationally explicable higher order structure formation.
- The repeating units of the supramolecular polymers and their polymerizable functions need to be arranged in a well-defined manner such that individual strands of the supramolecular polymers are unambiguously converted into single covalent polymer backbones.
- The applied polymerization methodology must be performed under conditions compatible with the self-assembly process and vice versa.
- The formation of the covalent polymer backbone should proceed under retention or, at least, controlled conversion of the previously self-assembled hierarchical structures; this requires, in particular, the structural requirements of the covalent capture process to be commensurate with the placement of the polymerizable functions in the self-assembled aggregates.

As our own investigations are specifically directed at the preparation of hierarchically structured polymers with  $\pi$ -conjugated backbones, we have chosen macromonomers based on  $\beta$ -sheet forming oligopeptide–polymer conjugates as the supramolecular scaffold and the UV induced topochemical diacetylene polymerization<sup>[9]</sup> as the polymerization methodology. The latter appears to be the method of choice because it is atom-efficient, initiator- and catalyst-free. Furthermore, it proceeds in the sense of a *trans*-stereospecific 1,4-polyaddition, and the obtained poly(diacetylene)s are  $\pi$ -conjugated, photoconductive polymers.<sup>[9]</sup> The polymerization is possible whenever diacetylenes are placed at an appropriate distance and packing angle. It is, therefore, not restricted to 3D single crystals, and research in the field has been reinvigorated with ideas from supramolecular chemistry and crystal engineering.<sup>[10]</sup> Topochemical diacetylene polymerizations have, for example, been performed in self-assembled mono-, bi- and multilayers and Langmuir–Blodgett films of diacetylene containing amphiphiles.<sup>[10a–c]</sup> Other types of self-assembled scaffolds have been employed, such as 1D lamellar structures in self-assembled monolayers on surfaces,<sup>[10d–f]</sup> columnar LC phases of discotic monomers,<sup>[10g–j]</sup> vesicles and related self-assembled structures in the submicron range,<sup>[10j–m]</sup> as well as organogels from hydrogen bonded 1D aggregates in solution.<sup>[10n–q]</sup>

In contrast to previous investigations, however, the targeted preparation of hierarchically structured poly(diacety-

lene)s with a defined, finite number of polymer strands requires the presence of equally well-defined, uniform supramolecular polymers<sup>[11]</sup> with the propensity to form predictable superstructures, instead of micellar or vesicular one-dimensional aggregates. As will be shown in the following sections,  $\beta$ -sheet forming oligopeptide–polymer conjugates have been proved to be reliable supramolecular synthons, giving rise to uniform nanoscopic aggregates with a high aspect ratio and the propensity to rationally explicable hierarchical structure formation in solution. As the packing distance between adjacent  $\beta$ -strands within a single  $\beta$ -sheet of  $d \approx 4.8 \text{ \AA}$  is close to the diacetylene packing distance of  $4.91 \text{ \AA}$  ideally required for a successful topochemical diacetylene polymerization, the chosen supramolecular scaffold and polymerization method appear to be mutually compatible and perfectly fulfil the above requirements.

### Lessons from the Formation of Amyloid Fibrils

As nature's way of self-organizing molecules into materials serves as the role model for the strategy toward hierarchically structured  $\pi$ -conjugated polymers outlined above, the best starting point for its development appears to be a look at nanostructures from  $\beta$ -sheet forming oligopeptides as they occur in biological systems. A prominent example of such structures are fibrous protein deposits termed "amyloids" which have received increasing attention in recent years because they are in one way or another associated with a number of severe diseases such as Alzheimer's, Parkinson's, and Huntington's disease, as well as various prion diseases and type II diabetes.<sup>[12]</sup> Their exact role in context with the associated diseases<sup>[12a,c]</sup> as well as the actual formation mechanism(s)<sup>[12d]</sup> are still a matter of debate, and different, sometimes conflicting structural models have been proposed for specific examples. There is, in fact, no evidence that all examples of amyloid fibrils need to be formed via the same mechanism or that their spines rely on exactly the same structural elements. By contrast, there are examples for different structure models, and different oligopeptide fragments from the same protein (or even one and the same oligopeptide under different conditions) may self-organize into different types of aggregates.<sup>[12b]</sup> Nevertheless, the formation of amyloid fibrils appears to follow a generic pattern in the sense that i) they are formed from a range of structurally non-related precursor proteins, ii) their internal structure is rich in  $\beta$ -sheet structures, and iii) their nanoscopic morphology is very similar. Thus, typical amyloid fibrils are helically twisted filaments of several micrometers in length and a width on the order of 10 nm. They exhibit a cross- $\beta$ -sheet signature in X-ray diffractograms with a  $4.7 \text{ \AA}$  meridional reflection and a broader equatorial reflection at a spacing of typically  $6\text{--}12 \text{ \AA}$ , which means that their spine structures most likely contain a finite number of stacked ("laminated") parallel or antiparallel  $\beta$ -sheets aligned in the direction of the fibril axis.<sup>[13]</sup>

In a number of important examples,<sup>[14]</sup> such as protofilaments from the full length amyloid protein A $\beta$  associated with Alzheimer's disease,<sup>[14a-c]</sup> from the yeast prion proteins Sup35p<sup>[14d]</sup> and Ure2p,<sup>[14e,f]</sup> or from human amylin associated with type II diabetes,<sup>[14g]</sup> the presence of stacked parallel, in-register  $\beta$ -sheets<sup>[15]</sup> has recently been conclusively established. In these specific examples, a terminal region of the precursor protein is folded into serpentine structures of  $\beta$ -strands<sup>[16]</sup> which then aggregate into parallel, in-register  $\beta$ -sheet structures such that the stacked  $\beta$ -sheets have an alternating  $\beta$ -strand directionality (Figure 3a-c). A somewhat different model has been proposed for fibrils from insulin<sup>[14h]</sup> where the three disulfide bonds place constraints on the molecular structure of the fibrils. Here, the two oligopeptide chains of the insulin molecule are assumed to rearrange their conformation and stack in a way that they form a pair of parallel  $\beta$ -sheets with opposite  $\beta$ -strand directionality which then further self-assemble into a variety of entwined

fibrils (Figure 3e,f). In other cases, parallel  $\beta$ -helix spine structures have been proposed,<sup>[17]</sup> and it appears that, until to date, antiparallel  $\beta$ -sheets have only been demonstrated in amyloid-like fibrils from relatively short oligopeptides composed of 15 residues or less.<sup>[12b]</sup> Interestingly, the somewhat surprising prevalence of parallel  $\beta$ -sheet structures has recently been correlated with the presence of specific amino acid sequences.<sup>[18]</sup> For example, the oligopeptide GlyAsnAsnGlnGlnAsnTyr **2** in the  $\beta$ -sheet forming domain of the yeast prion protein Sup35p has been shown to form tight pairs of parallel, in-register  $\beta$ -sheets with opposite strand directionality.<sup>[18a]</sup> The dimerization proceeds under complete exclusion of solvent molecules and is based on both the self-complementary topology of the resulting  $\beta$ -sheet surfaces and the presence of the Asn and Gln side chain amide groups as, likewise, self-complementary hydrogen bond donors and acceptors (Figure 4). These are arranged in such a way that an efficient interstrand, intrasheet hydrogen

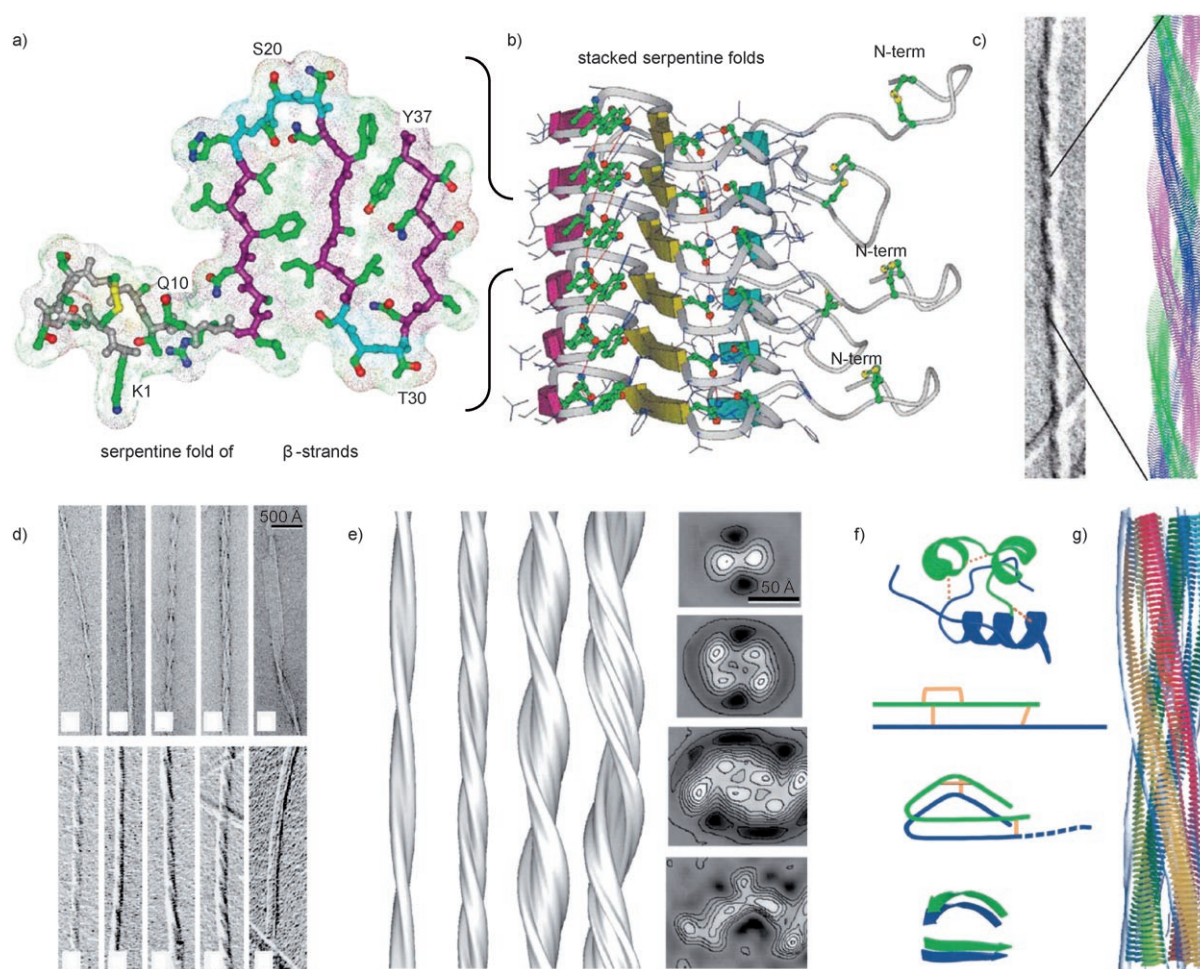


Figure 3. Representative examples of TEM images and proposed structural models for amyloid fibrils from (a-c) human amylin and (d-f) insulin; a) proposed serpentine fold with three  $\beta$ -strands from human amylin; b) protofilament model showing a stack of these serpentine folds; c) electron micrograph of a human amylin fibril (shadowed) and a model consisting of three entwined protofilaments; d) a variety of negatively stained (top) and shadowed (bottom) left-handed helical filaments from insulin; e) surface representation of 3D maps and contoured density cross-sections of these insulin filaments; f) the native conformation of the two insulin chains (green, blue) can be rearranged into two pairs of parallel  $\beta$ -strands which stack to form the protofilaments; g) a model of three entwined protofilaments overlaid with a TEM density map (transparent gray surface). Reproduced with permission from ref. [14g,h].

bonding can only be realized in case of a parallel, in-register  $\beta$ -strand orientation within the  $\beta$ -sheets. This structural motif has been termed a “dry steric zipper”, and a whole range of related structures have recently been described and associated with amyloid fibril formation.<sup>[18b]</sup>

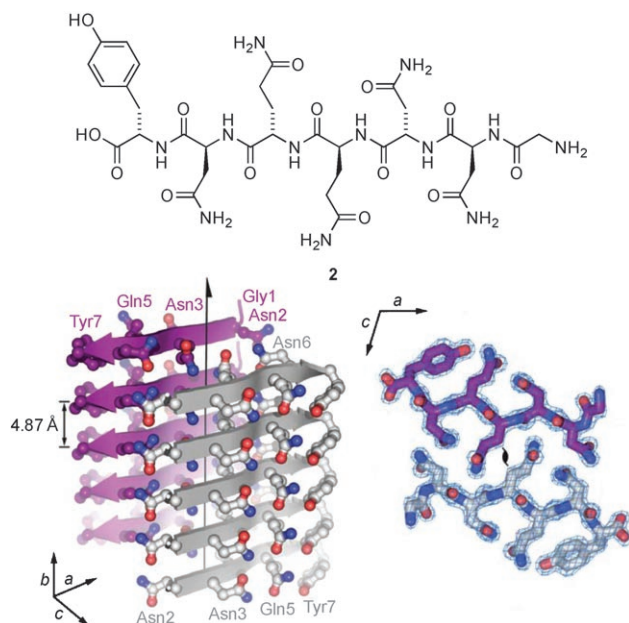


Figure 4. Crystal structure of the dry steric zipper observed in fibrils of the oligopeptide GNNQQNY **2** from the spine structure of the yeast prion protein Sup35p; a pair of parallel  $\beta$ -sheets (gray, purple) forms under exclusion of solvent due to the self-complementary topology (compare cross-section on the right) and hydrogen bonding sites in the side chain amides. Reproduced with permission from ref. [18a].

Looking at the process of amyloid fibril formation with the eyes of a polymer chemist and leaving aside both the diversity and complexity of biological structures for a moment, an analogy to rod-coil block copolymers comes to mind. It looks like the prerequisite for the formation of well-defined, high aspect ratio filaments relies on some sort of “phase segregation” between, on one side, the  $\beta$ -strands as relatively short, monodisperse, and preorganized crystallizable segments and, on the other side, the connecting turns and loops as well as the remainder of the proteins, all of which create a “soft shell” around the filaments.<sup>[19]</sup> It may seem trivial to state that the crystallization of the former is the driving force for fibrillization for which reason it may not come as a surprise that proteins with natively disordered terminal domains constitute an important family of amyloidogenic proteins. However, a less obvious conclusion is that the soft shell around the crystalline core also plays a crucial role in that it helps to provide sufficient solubility to allow for a fast aggregation into well-defined, high aspect-ratio one-dimensional aggregates and prevents the premature precipitation of insoluble polycrystalline assemblies. Of course, the obtained fibrils are, ultimately, completely insoluble. This and the fact that comparably large oligopeptide

segments have to be appropriately folded as the first step of self-assembly probably render amyloid based systems themselves too complex to be utilized as supramolecular scaffolds in synthetic chemistry. However, it would be a sufficient simplification if short, linear oligopeptides could be utilized to form  $\beta$ -sheets, and synthetic polymer segments would be employed in order to take over the role of the globular domains attached to the fibrils' core, even enhance phase segregation, and provide improved solubility in a larger range of protic or aprotic solvents.

### Defined Nanoscopic Aggregates from Designed Short Oligopeptides and Peptidomimetics

As a first step in this direction, the self-organization of short, linear oligopeptides into  $\beta$ -sheets and higher structures has to be thoroughly understood. The situation is different from the self-assembly of amyloid fibrils in one important aspect; the individual  $\beta$ -strands are not folded into arrangements that yield several stacked  $\beta$ -sheets at once, so that the stacking of these  $\beta$ -sheets becomes an independent process. Boden and co-workers investigated the hierarchical self-organization of the 24-residue oligopeptide K24 derived from the  $\beta$ -sheet forming domain of a transmembrane protein as well as a set of de novo designed 11-residue oligopeptides.<sup>[20]</sup> These oligopeptides were found to undergo a step-wise self-organization into distinct types of uniform, left-handed helical, nanoscopic 1D aggregates which the authors described as curled single  $\beta$ -sheet tapes, twisted ribbons (double tapes), fibrils (stacked ribbons), as well as fibers (entwined fibrils). Based on their experimental findings, Boden, Fishwick et al. rationalized the observed hierarchical self-organization in a remarkably intuitive generalized model (Figure 5).<sup>[20b]</sup> Thus, they assumed that the oligopeptide strands attained a chiral rod conformation with a right-handed helical twist originating from the L-chirality of the natural amino acids. The molecules would then self-assemble into single antiparallel  $\beta$ -sheet tapes with different left-handed helical superstructures, depending on the nature of the tapes' surfaces. For instance, if the tapes' surfaces are amphiphilic, the tapes will tend to “curl” into tubular left-handed helices in order to hide the more hydrophobic surface inside. Alternatively, they may form ribbons (double tapes) via  $\beta$ -sheet stacking for the same purpose. These ribbons undergo further  $\beta$ -sheet stacking via their more hydrophilic surfaces to yield fibrils; and the latter may, finally, form fibers via edge-to-edge attraction.<sup>[21]</sup>

The most important implication of this model is that distinct types of supramolecular interactions with significantly different energies are associated with each level of self-organization.<sup>[20b]</sup> The self-assembly into single  $\beta$ -sheet tapes occurs due to N-H...O=C type hydrogen bonding. By contrast, both the  $\beta$ -sheet stacking of tapes into ribbons via the more hydrophobic  $\beta$ -sheet surfaces as well as the subsequent stacking of ribbons into fibrils via the more hydrophilic surfaces will depend on the chemical nature and the topology

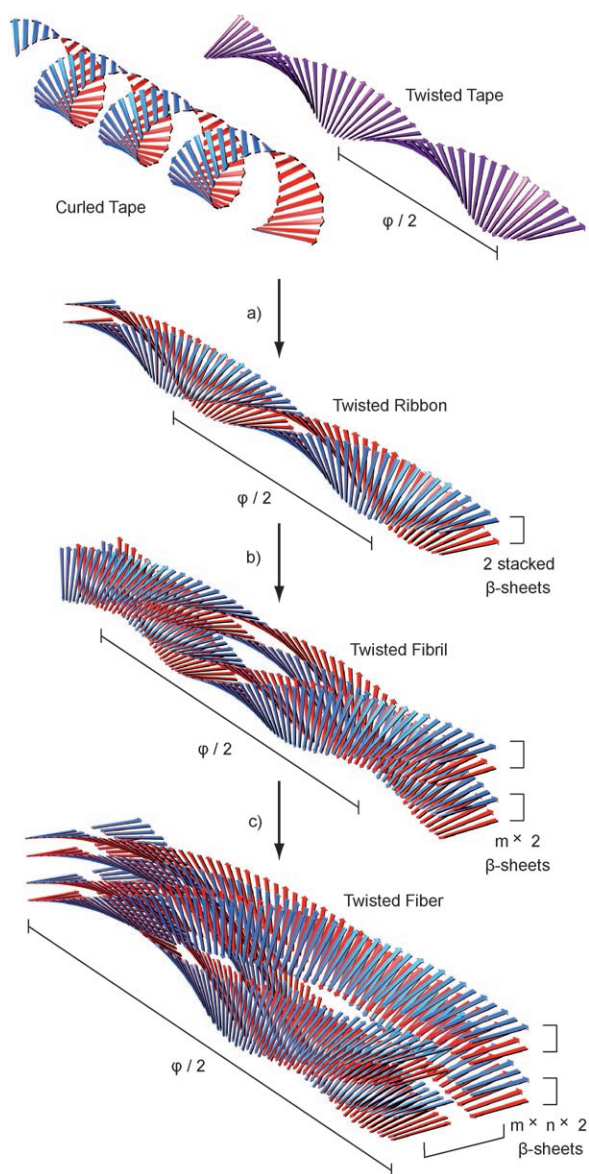


Figure 5. Schematic summary of Boden's model for the step-wise hierarchical self-organization of oligopeptides in protic media; depending on the amino acid sequence, oligopeptides will aggregate into a) single  $\beta$ -sheet tapes with different helical superstructures; b) amphiphilic tapes will dimerize into ribbons via  $\beta$ -sheet stacking, hiding the more solvophobic surfaces; c) ribbons may further stack into fibrils which can further aggregate into fibers via edge-to-edge attraction.

of the involved surfaces and may be mediated by diverse kinds of interactions, for example, hydrogen bonding, electrostatic, van der Waals, or repulsive steric interactions. However, the former process is expected to be supported by the hydrophobic effect and will, typically, be significantly more favorable than the latter. Finally, fiber formation will strongly depend on the exact chemical nature of the  $\beta$ -sheets' edges and, again, be significantly less favorable than the other processes. In conclusion, the distinct levels of self-organization are associated with what may be regarded as an orthogonal set of interactions, all of which may be ad-

ressed individually by changing the molecular structure or the chemical environment.

Secondly, it is the inherent helical twisting of  $\beta$ -sheet based fibrillar aggregates on all levels of self-organization which is the main factor responsible for the formation of uniform 1D aggregates with a defined and finite number of laminated  $\beta$ -sheet tapes.<sup>[20b]</sup> The observed helical pitch  $\phi$  of the final aggregate is a mere compromise in order to maintain the N-H...O=C hydrogen bond connectivity between all amino acid residues in all  $\beta$ -strands of all incorporated  $\beta$ -sheet tapes. Thus, increasing the number of laminated tapes must lead to an unwinding of the helical twist until it completely disappears in a whole layer of infinitely stacked  $\beta$ -sheets. Likewise, increasing the length of the constituent oligopeptide  $\beta$ -strands will result in a decreased  $\beta$ -sheet twisting. Assuming that there is an optimal degree of twisting for individual  $\beta$ -strands of a given length and chemical structure, the unwinding process must be associated with an elastic energy penalty which counteracts and, at a certain point, compensates the enthalpy gain associated with  $\beta$ -sheet stacking, prohibiting an "unlimited"  $\beta$ -sheet lamination.

In summary, it is the interplay of the significantly different aggregation enthalpies on the distinct levels of self-organization combined with the energetic penalty associated with re-adjusting the helix geometry upon aggregation that controls the formation of well-defined aggregates with a finite number of laminated tapes and, consequently, a finite diameter. The result is a uniform thermodynamic equilibrium structure with a defined, finite number of laminated  $\beta$ -sheets that can be fine-tuned by a judicious choice of the oligopeptide's molecular structure. While this model provides an elegant explanation for most aspects of oligopeptide self-organization, it should be critically noted that the implications of parallel  $\beta$ -sheet formation as well as the role of the  $\beta$ -sheets' residual dipole moment components in general have not been explicitly considered.<sup>[22]</sup>

### Nanoscale Scaffolds from Oligopeptide-Polymer Conjugates

The above examples serve to highlight that pure oligopeptides are versatile supramolecular scaffolds. Nevertheless, moving toward oligopeptide-polymer conjugates significantly enlarges their scope, in particular with respect to the accessible chemical environments. Furthermore, the decoration of the  $\beta$ -sheet tape edges with polymer segments will introduce an element of phase segregation unknown in the realm of pure oligopeptides which will strongly favor the formation of filaments with a lower number of laminated sheets and disfavor bundle formation. Aggregation via  $\beta$ -sheet stacking would successively restrict the space available to the attached polymer segments, and the required chain extension would only be thermodynamically favorable if the associated entropic penalty was overcompensated by an enthalpic contribution, for example, from a crystallization of

the polymer segments. Hence, while the general considerations concerning the self-assembly of oligopeptides remain valid, the attachment of *amorphous* polymer segments to the tape edges plays a role similar to the “soft shell” of amyloid proteins or, for instance, electrostatic repulsion in the case of pure oligopeptides, although the thermodynamic origin of the effect is different, that is, entropic in nature.

The following representative examples will help to demonstrate that polymer attachment provides solubility in the chosen solvent and helps to promote the well-defined supramolecular aggregation into high aspect ratio filaments without premature precipitation of ill-defined insoluble material.<sup>[23]</sup> Lynn et al., for instance, investigated PEO conjugates of the  $\beta$ -sheet forming fragment A $\beta_{10-35}$  of the  $\beta$ -amyloid protein associated with Alzheimer's disease.<sup>[23a-c]</sup> This example is illustrative because it allows for a direct comparison of the pure amyloidogenic oligopeptides (see above) and their polymer conjugates. The authors observed a reversible, pH dependent aggregation into parallel  $\beta$ -sheet structures accompanied with the formation of nanoscopic helical fibrillar features similar to the ones obtained from the pure oligopeptide and other amyloidogenic oligopeptides (see above). The fibrils exhibited a core diameter of about 9 nm, a large superhelical pitch of 110 nm, and appeared to consist of about six laminated  $\beta$ -sheets. However, in marked contrast to the pure oligopeptides, the PEO conjugates did not exhibit any tendency to form fibril bundles. This factor, consequently, appeared to be the key element to avoid the irreversible formation of insoluble material. In contrast to the supposedly folded amyloid fragment used in the preceding example, Börner et al. investigated the self-assembly of the probably unfolded PEO-NH-Gly(ValThr)<sub>5</sub>TrpGly-NH<sub>2</sub> **3**.<sup>[23d]</sup> The molecules featured an amino acid sequence that gives rise to antiparallel  $\beta$ -sheet tapes with strongly amphiphilic surfaces and formed extremely long microfibers instead of nanoscopic aggregates, with a surprisingly narrow diameter of  $2.0 \pm 0.5 \mu\text{m}$  and a height of about  $50 \pm 5 \text{ nm}$  (Figure 6a). The authors proposed these microfibers to comprise a large number of laminated  $\beta$ -sheets running parallel to the fiber axis and stacked perpendicular to their long diameter. Nanoscopic filaments were obtained, on the other hand, when either a shorter oligopeptide segment was employed or the significance of the  $\beta$ -sheet surfaces' amphiphilicity was reduced by changing to an organic solvent. While the shorter linear PEO-NH-(ValThr)<sub>4</sub>C(O)CH<sub>2</sub>NMe<sub>2</sub> **4** did not show any tendency toward fibrillization at all, the peptidomimetic molecules **5**<sup>[24]</sup> as well as the closely related polymer conjugates **6**,<sup>[23e]</sup> which comprise two ValThrValThr strands linked with a dibenzofuran and a PEO-substituted carbazole moiety, respectively, both gave rise to defined nanoscopic aggregates.<sup>[25]</sup> Thus, the conjugates **6** were found to produce uniform nanoscopic ribbons with a height of  $1.4 \pm 0.1 \text{ nm}$  and a lateral spacing of closely packed ribbons of  $13.6 \pm 1 \text{ nm}$  (Figure 6b). Again, they showed no tendency to form higher aggregates such as bundles, as opposed to filaments from the pure peptidomimetic molecules **5**. Similarly, the poly(butyl acrylate) equipped pBuA-C(O)NH-(Val-

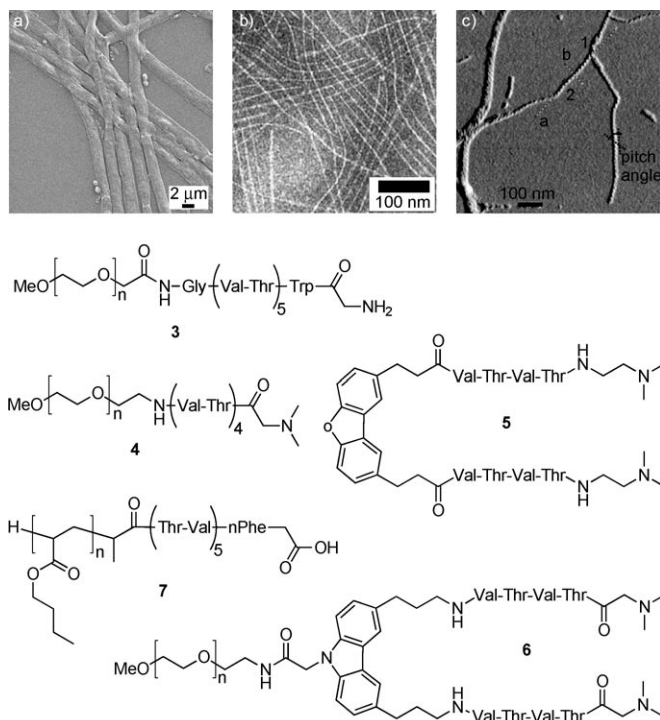


Figure 6. a) SEM micrograph of the microfibers obtained from **3**; b) TEM image (negative stain) of nanoscopic filaments observed in the case of **6**; c) SFM image of helical nanoscopic filaments self-assembled from **7**. Reproduced (in part) with permission from ref. [23d-f].

Thr)<sub>5</sub>-nPheGlyOOH **7** (nPhe = 4-nitrophenylalanine) self-assembled into left-handed helically twisted nanoscopic filaments with a height of  $2.9 \pm 0.5 \text{ nm}$ , a helix pitch of  $37.4 \pm 3 \text{ nm}$ , and lengths of up to  $2.3 \mu\text{m}$  (Figure 6c).<sup>[23f]</sup>

### A Set of Guidelines for the Construction of Scaffolds from Oligopeptide–Polymer Conjugates

Summarizing the above examples and conclusions from the self-organization of oligopeptides and their polymer conjugates, the following set of guidelines can be derived for their design and utilization as nanoscopic supramolecular scaffolds.

- In aprotic organic solvents, the formation of stable single  $\beta$ -sheet tapes can be achieved with shorter oligopeptide segments because the N-H $\cdots$ O=C-type hydrogen bonding is stronger in the absence of competition from the solvent.
- Single  $\beta$ -sheet tapes from shorter oligopeptides are expected to favor a stronger helical twisting and, therefore, disfavor higher aggregation via  $\beta$ -sheet stacking. This may, hence, favor tape over ribbon over fibril formation, or at least lead to filaments with a lower number of laminated  $\beta$ -sheets.
- The mutual attraction of  $\beta$ -sheets should, in general, be noticeably reduced in apolar solvents as compared to



protic media due to the absence of the hydrophobic effect. This should favor systems with a lower number of laminated  $\beta$ -sheets.

- An alternating sequence of hydrophilic and hydrophobic amino acids leads to amphiphilic tape surfaces, which will selectively favor the dimerization of tapes into ribbons and suppress higher aggregation, irrespective of the environment.<sup>[26]</sup>
- The inclusion of additional repulsive (e.g., electrostatic) interactions will selectively favor tape (or ribbon) formation over higher aggregation via  $\beta$ -sheet stacking (depending on their actual placement along the  $\beta$ -sheet surfaces).
- The steric repulsion of non-crystalline polymer segments attached to the  $\beta$ -sheet surfaces or edges may serve a similar purpose. Due to the entropic nature of this effect, increasing the length of the polymer segments should favor systems with a lower number of laminated  $\beta$ -sheets.

### How To Enforce Parallel versus Antiparallel Aggregation

For the envisaged topochemical diacetylene polymerization using self-assembled oligopeptide fibrils as scaffolds, the polymerizable diacetylene moieties must be placed in-register at the intersheet  $\beta$ -strand identity period of around 4.8 Å. An antiparallel  $\beta$ -strand arrangement would, hence, be detrimental, and a viable strategy to achieve parallel  $\beta$ -sheet formation is needed. Considering the prevalence of  $\beta$ -sheet-rich proteins with parallel  $\beta$ -sheet structures in nature, it may seem a little disappointing that more or less all investigations on synthetic oligopeptides and their polymer conjugates either quietly assumed, experimentally observed, or deliberately targeted predominantly antiparallel  $\beta$ -sheet formation. With the exception of Lynn's and Meredith's investigations on PEO conjugates of amyloidogenic oligopeptides which exhibited the same parallel  $\beta$ -sheet structure as the unmodified amyloid proteins, there is, to the best of our knowledge, not a single example of a synthetic oligopeptide or its polymer conjugate which was specifically designed for parallel  $\beta$ -sheet formation. In this context, it is important to acknowledge that, for simple oligopeptides, an antiparallel  $\beta$ -strand orientation should usually be preferred because of the favorable compensation of the molecular dipoles and the more optimal hydrogen bond geometries. Furthermore, it can straightforwardly be enforced by including additional complementary interaction sites in the side chains or at the  $\beta$ -strand termini, as it has been done in the above examples by Boden, Kelly, or Börner.

While no similarly straightforward method to enforce parallel  $\beta$ -sheet formation has previously been described, the simple inclusion of appropriately placed complementary interaction sites (e.g., pairs of acid/base, hydrogen bond donor/acceptor, or cationogenic/anionogenic functionalities) should be expected to give rise to a parallel  $\beta$ -strand align-

ment only if two different, mutually complementary types of molecules are employed and co-assembled (Figure 7a). An alternative strategy may be the attachment of two different, non-miscible polymer segments to the oligopeptide termini, which would favor a parallel aggregation due to phase segregation. Finally, a desymmetrization of the interactions responsible for  $\beta$ -sheet formation such as, for instance, a non-equidistant placement of the N-H...O=C backbone hydrogen bonding sites by including a non-peptidic spacer, can be envisaged to induce parallel  $\beta$ -sheet formation because, only in this way, the maximum number of hydrogen bonds can be achieved. It is interesting to note that this last strategy appears to be closely related to how parallel  $\beta$ -sheets are obtained in biology; the described "dry steric zipper" motif (see above) frequently observed in amyloid fibrils incorporates additional, self-complementary side chain N-H...O=C type hydrogen bonding sites placed in a way that the stabilizing interstrand, intrasheet hydrogen bonding can only be realized in a parallel  $\beta$ -sheet structure (Figure 4). The re-

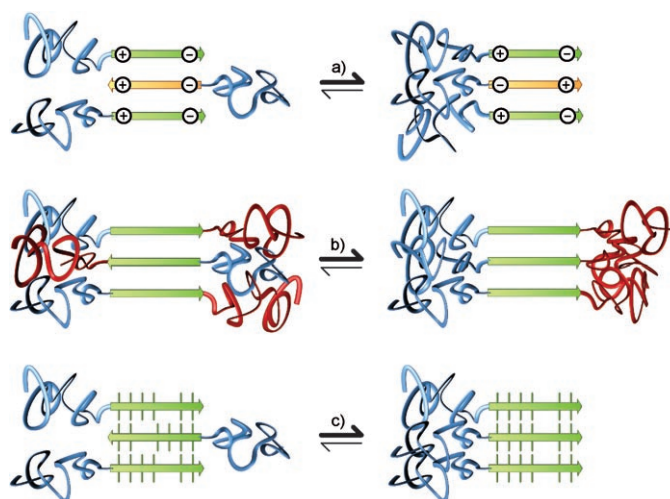


Figure 7. Possible strategies to enforce a parallel  $\beta$ -strand orientation; a) the inclusion of complementary interaction sites requires the preparation of two different, mutually complementary molecules; b) oligopeptides equipped with two different, immiscible polymer segments may favor a parallel orientation due to phase segregation; c) likewise, the non-equidistant placement of N-H...O=C backbone hydrogen bonding sites or additional side chain interaction sites may induce parallel alignment.

cently demonstrated generic nature and abundance of this motif in fibrous proteins makes this last strategy seem most promising for its utilization in the preparation of self-assembled scaffolds for the topochemical diacetylene polymerization.

### Self-Assembly of Diacetylene Macromonomers Based on Oligopeptide-Polymer Conjugates

Macromonomers **8–12** (Figure 8) were designed on the basis of the above guidelines and considerations.<sup>[27]</sup> Thus, they in-

incorporated a hydrogenated poly(isoprene) segment as a non-crystalline, flexible, hydrophobic polymer segment; tetra(L-alanine) as a simple, short, and hydrophobic oligopeptide aggregator in order to allow for self-assembly in organic media; a diacetylene moiety as the polymerizable function; and a variety of hydrogen bonded end groups. As the strand direction in these end groups was chosen to be the same as in the aggregator segment, the diacetylene moieties themselves may be regarded as rigid, non-peptidic spacers directly incorporated into the N-H...O=C backbone hydrogen bonding array, separating the latter into two unequal sections. Of course, any contribution from the additional hydrogen bonds in favor of a parallel  $\beta$ -strand competes with other factors (e.g., steric repulsion of the attached polymer segments) and the outcome must, hence, be expected to depend on the number of additional hydrogen bonds and their strength. Therefore, derivatives **13–16** were synthesized as a control to investigate the role of the hydrogen bonding sites in the end groups.

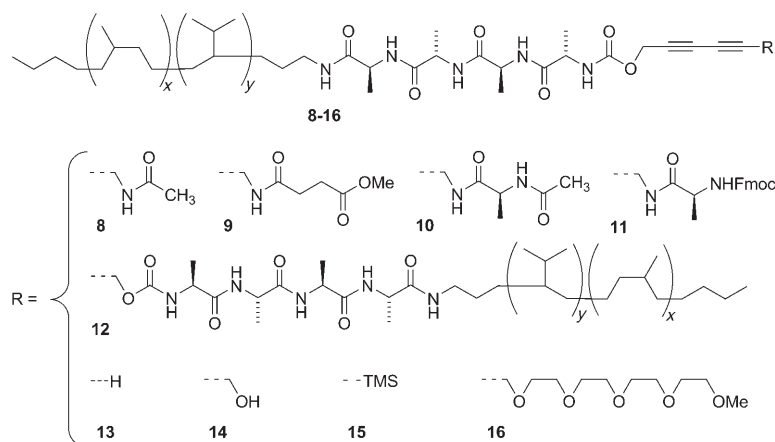


Figure 8. Diacetylene macromonomers substituted with oligopeptide–polymer conjugates and different end groups ( $P_{x+y} \approx 10$ , and a ratio of  $x/y \approx 0.2$ ).

All derivatives were synthesized from amine terminated poly(isoprene) by high pressure hydrogenation, sequential peptide coupling reactions, and a final coupling to different amino acid substituted diacetylene building blocks. The solution phase IR spectra in  $\text{CH}_2\text{Cl}_2$  in combination with solid state REDOR and DOQSY NMR experiments on  $^{13}\text{C}$  and  $^{15}\text{N}$  labelled compounds allowed to conclude that derivatives **8–14** exhibited the expected predominant formation of  $\beta$ -sheet secondary structures, whereas mixtures with other structures were observed for **15** and **16**.<sup>[28]</sup> The particularly clear IR signature of macromonomers **8–12** implied a high degree of  $\beta$ -sheet formation and internal order. More importantly, however, a detailed comparison revealed systematic and distinct differences between these macromonomers and the other compounds. Thus, an unusual combination of amide I and amide II bands was observed and found to be similar to calculated values of hypothetical parallel single  $\beta$ -

sheet structures.<sup>[27]</sup> By contrast, **13** and **14** exhibited both amide I and amide II bands in excellent agreement with the presence of antiparallel  $\beta$ -sheets.

SFM imaging proved that the number and pattern of the  $(5+x)$  N-H...O=C type hydrogen bonding sites strictly controlled both the stability of the  $\beta$ -sheet aggregates and their superstructures.<sup>[27]</sup> Thus, macromonomers **8–12** self-organized into many micrometers long fibrillar features with a persistence length estimated to be significantly beyond 100 nm (Figure 9). By contrast, compounds **13** and **14** gave rise to much shorter and more flexible flat tapes together with substantial amounts of non-fibrillar material (not shown), and only non-fibrillar material was observed in the case of **15** and **16**. Interestingly, the filaments produced by macromonomers with the same number and pattern of hydrogen bonds turned out to be very similar in morphology. For example, **8** and **9** with  $(5+1)$  hydrogen bonds both produced fibrils which could be identified as right-handed double-helical fibrils with a uniform apparent height and an

estimated width on the order of 5–6 nm as well as a periodicity of about 18 nm (i.e., a helix pitch of about 36 nm). The helices were constituted from two flat ribbon substructures which had a width on the order of about twice the molecules' extended length. By contrast, macromonomers **10** and **11**, which comprise  $(5+2)$  hydrogen bonding sites, gave rise to uniform left-handed single-helical ribbons which exhibited a complex fine structure with a periodicity of approximately 120 nm and were tentatively interpreted as curled and twisted helices. Finally, SFM images of the symmetric dimer **12**, exhibiting  $(5+5)$  hydrogen bonds, revealed

the presence of smooth, flat, and very rigid tapes with an apparent height of about 2.5 nm and an approximate width of 7 nm, that is, a little less than the extended length of one molecule.

The experimental findings can straightforwardly be rationalized on the basis of Boden's model extended toward oligopeptide–polymer conjugates with hydrophobic polymer segments in organic solution (see above) if the effects of parallel  $\beta$ -sheet formation are considered.<sup>[27]</sup> Thus, the formation of comparably stable single  $\beta$ -sheet tapes may be safely assumed as the first step in the self-organization of all macromonomers and derivatives. As a result, both edges of single antiparallel  $\beta$ -sheet tapes from compounds **13–16** will be lined with the hydrophobic polymer segments, and the oligopeptides' inherent dipole moment components in  $\beta$ -strand direction cancel each other out (Figure 10b). Consequently, this mode of assembly may be referred to as apolar. The at-

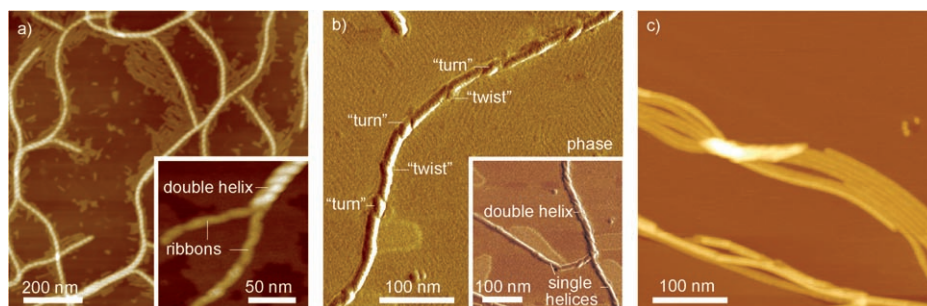


Figure 9. Representative examples of SFM images of the diacetylene macromonomers; a) **8** formed right-handed double-helical fibrils with an apparent height of  $5.8 (\pm 0.4)$  nm and a periodicity of  $18.1 (\pm 1.0)$  nm; b) **10** gave rise to left-handed single helices which only occasionally formed bundles and had a complex periodic fine structure with an identity period of  $120 (\pm 18)$  nm; c) SFM images of **12** showed flat tapes with an apparent height of  $2.5 (\pm 0.3)$  nm and an approximate width of about 7 nm.<sup>[27]</sup>

tached polymer segments can completely wrap the whole tape into a “hydrophobic cushion”, shielding the polar oligopeptide core from the hydrophobic environment. As the chosen hydrogenated poly(isoprene) segments are unable to pack due to their non-uniformity in molecular weight, tacticity and branching, any sort of  $\beta$ -sheet stacking will be rendered unfavorable. In the case of the symmetric dimer **12**, which contains two oligopeptide segments with opposite directionality covalently attached to the central diacetylene unit, the obtained single parallel  $\beta$ -sheet tapes incorporate two separate  $\beta$ -sheet domains with an *opposite*  $\beta$ -strand orientation (Figure 10a). As a result, the mode of aggregation is also apolar because the different domains’ dipole moment components perpendicular to the tape axis cancel out and both tape edges are equally decorated with hydrophobic polymer segments. Accordingly, a further organization into higher structures via  $\beta$ -sheet stacking is, again, unfavorable. Of course, the resulting tapes are wider as compared to the ones formed by **13–16** and also substantially more rigid because of the doubled number of hydrogen bonds.

A more complex situation is encountered in the case of macromonomers **8–11** because the formation of single  $\beta$ -sheet tapes with a parallel  $\beta$ -strand orientation leaves only one tape edge decorated with polymer chains whereas the other one is bare, leading to a steric mismatch. Furthermore, the tapes obtained have a net dipole component perpendicular to the tape axis so that the mode of self-assembly can be regarded as *polar* (Figure 10c). Finally, a simple molecular model helps to illustrate that the chosen chain length of  $P_n \approx 10–12$  of the attached hydrogenated poly(isoprene) segments is too short to wrap the entire tapes and, thus, shield the polar cores from the hydrophobic environment. The combination of these factors is believed to induce the formation of ribbons composed of two (partially) stacked tapes with opposite  $\beta$ -strand orientation (Figure 10d).

The origin of the observed differences between the superstructures of **8** and **9**, on one side, as well as **10** and **11**, on the other side, is less obvious. One reason may be the fact that the helically bent and twisted ribbons from **10** and **11** are held together by  $(5+2)$  hydrogen bonds per tape and

may, consequently, be too stiff to easily accommodate a further aggregation into fibrils (Figure 10e). By contrast, the smaller number of  $(5+1)$  hydrogen bonds in the ribbon substructures formed from **8** and **9** may provide just enough flexibility to accommodate double helix formation (Figure 10f). The presence of residual dipole moments in tape direction as a consequence of the *even* or *uneven* numbers of N-H $\cdots$ O=C hydrogen bonding sites on either side of the diacetylene spacer may be an additional

contributing factor the implications of which are difficult to assess.

### Topochemical Polymerization—From Supramolecular Assemblies to Conjugated Polymers

Upon UV irradiation in solution, macromonomers **8–12** were converted into the corresponding poly(diacetylene)s, whereas derivatives **13–16** did not undergo a polymerization at all.<sup>[27]</sup> UV spectra (Figure 11c) proved the successful poly(diacetylene) formation which was further corroborated with solid state  $^{13}\text{C}$  NMR as well as Raman spectroscopy on dried samples after polymerization. Hence, the UV induced polymerization also served as a sensitive probe for the internal structure of the self-assembled aggregates and helped to unambiguously confirm the interpretation of the IR spectra. Apparently, the presence of additional N-H $\cdots$ O=C type hydrogen bonding sites in the molecules’ end groups was an indispensable prerequisite for their topochemical polymerizability, in agreement with the assignment of the corresponding signature in the IR spectra to the presence of parallel  $\beta$ -sheet secondary structures. Interestingly, the order of reactivity was strictly determined by the total number  $(5+x)$  of hydrogen bonding sites in the macromonomers, with macromonomer **12** exhibiting the highest initial reactivity of all macromonomers, followed by **11**, **10**, **9**, and **8**. As expected for a chiral, helical conjugated polymer, the backbone chromophores exhibited CD activity. SFM imaging provided further evidence for the successful conversion of the supramolecular polymers into covalent, conjugated polymers under retention of their hierarchical structure. First of all, SFM images obtained from any of the polymerizable macromonomers **8–12** looked virtually identical before or after polymerization. The addition of a small amount of a deaggregating cosolvent such as hexafluoroisopropanol (HFIP) to the sample solutions in  $\text{CH}_2\text{Cl}_2$  before the UV irradiation led to a complete disappearance of fibrillar structures. By contrast, intact fibril sections with helical fine structure and

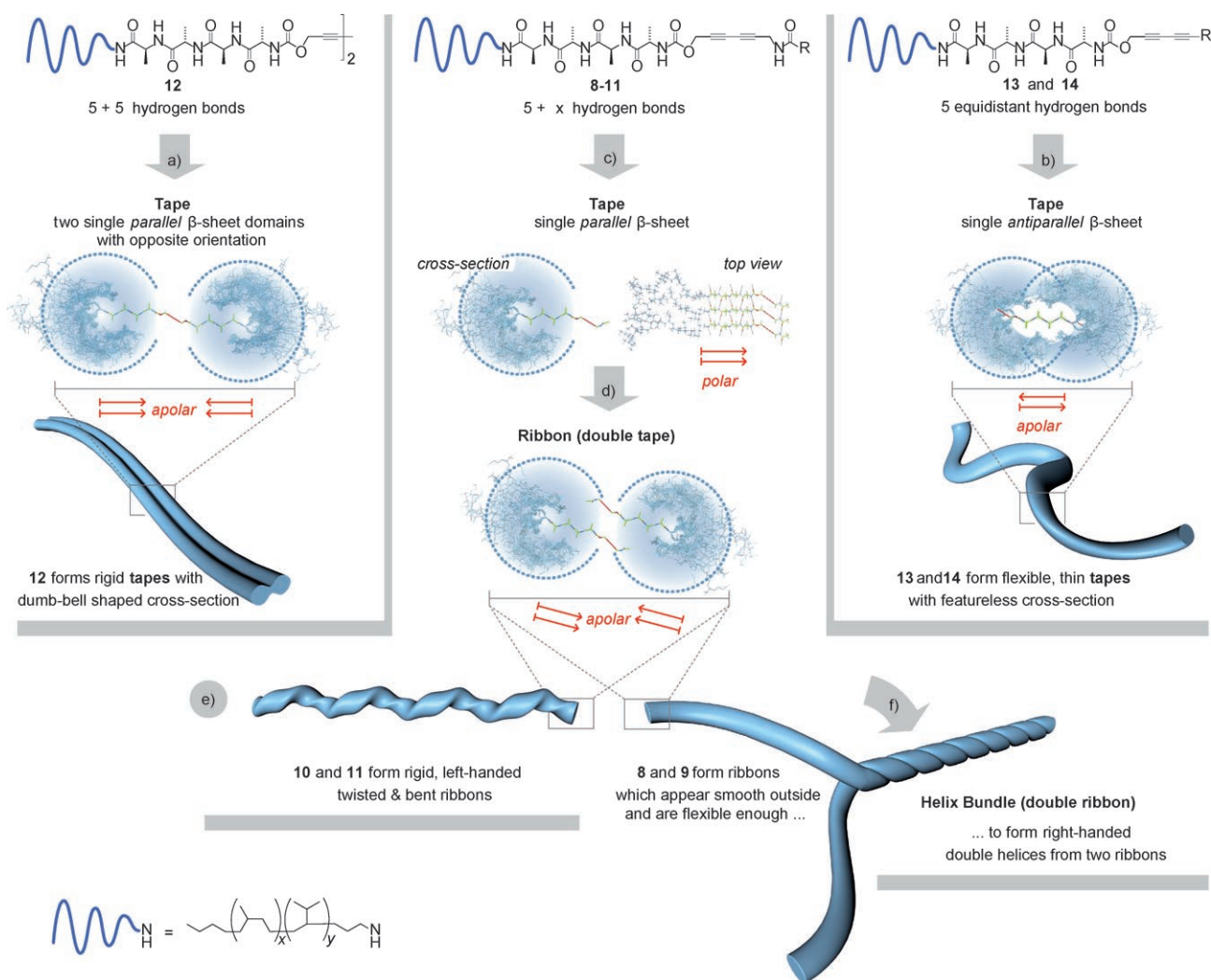


Figure 10. Model for the hierarchical self-organization of **8–16**; a) **12** forms tapes comprising two covalently linked single parallel  $\beta$ -sheet domains with opposite orientation; b) **13** and **14** aggregate into more flexible and less stable single antiparallel  $\beta$ -sheet tapes; c) tapes obtained by parallel  $\beta$ -sheet formation from **8–11** are polar structures which d) further self-organize into ribbons; e) left-handed twisted and bent ribbons from **10** and **11** are more rigid in comparison to f) ribbons from **8** and **9** which are flexible enough to form double-helical fibril bundles.<sup>[27]</sup>

an average contour length beyond 100 nm remained after UV irradiation (Figure 11a,b). Furthermore, these fibrils could be manipulated with the SFM tip, in contrast to the self-assembled fibrils before the UV-induced polymerization (Figure 11d–f).<sup>[27]</sup>

## Conclusion

In conclusion, oligopeptide-polymer conjugates are reliable supramolecular synthons for the formation of defined supramolecular assemblies which exhibit hierarchical structure formation. The latter can be rationalized (although not yet fully predicted) on the basis of structure models derived from both investigations of amyloid fibrils and designed synthetic oligopeptides, if the role of the attached polymer segments is taken into consideration. Thus, the aggregates' uniformity on the nanoscopic level is attributed to the complex

interplay of the oligopeptides' crystallization enthalpy, the elastic energy of helix pitch adjustment, and the grafted polymer segments' chain extension entropy. The superstructural diversity and, more explicitly, the molecular level control over secondary and higher structure formation as well as polymerizability can be rationalized to result from a simple set of parameters, that is, the non-equidistant placement, the exact distribution, and the total number of N-H $\cdots$ O=C type hydrogen bonding sites in the macromonomers. Hence, supramolecular self-assembly and covalent capture by topochemical polymerization were utilized as supramolecular-synthetic methods, complementing traditional organic- and polymer-synthetic methods, in order to prepare a new class of functional, soluble poly(diacetylene)s.

As the constituting single  $\beta$ -sheet tapes can be regarded as supramolecular polymers, the observed tapes, ribbons, and fibrils were uniform supramolecular polymers with a defined, finite number of polymer strands corresponding to

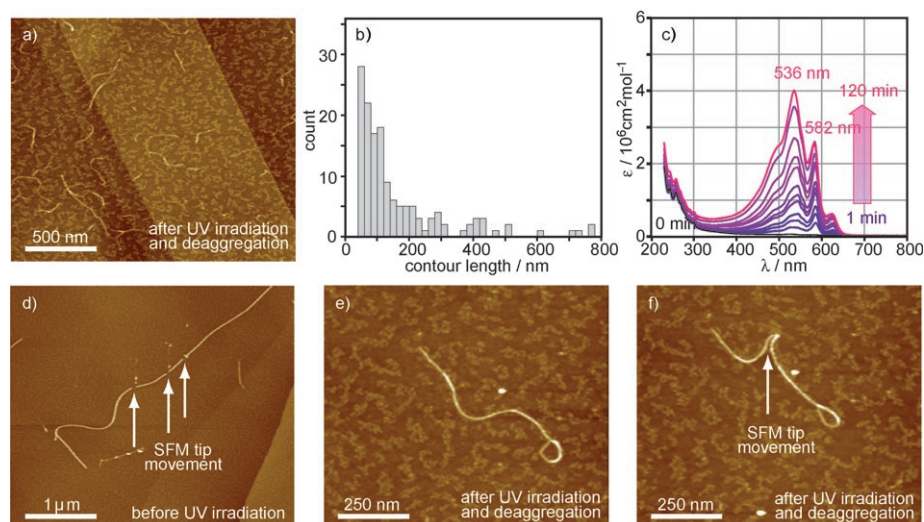


Figure 11. UV induced topochemical polymerization of the self-assembled filaments from **9** as a representative example; a) upon addition of HFIP to a sample solution in  $\text{CH}_2\text{Cl}_2$  after UV irradiation, helical fibrillar features of b) up to several hundred nanometers in length remained intact; c) UV spectra proved the poly(diacetylene) formation; d) manipulation with the SFM tip destroyed the non-irradiated self-assembled fibrils from **9**; but e, f) SFM tip manipulation was possible after UV induced polymerization.

the number of stacked  $\beta$ -sheet tapes, rather than micellar or vesicular structures. Hence, their conversion into covalent, conjugated polymers by topochemical diacetylene polymerization yielded multi-stranded conjugated polymers with equally well-defined single-stranded, double-helical, or quadruple helical quaternary structures which only find an analogy in biopolymers. The detailed understanding of the underlying self-assembly processes will allow to prepare multifunctional conjugated polymers with designed superstructures and justifies the applied approach to be considered as a viable general strategy toward such polymer architectures which complements the already successful foldamer concept.

## Acknowledgements

The authors would like to thank Professor Jürgen Rabe and Dr. Nikolai Severin for the fruitful cooperation, Dr. Jeroen van Heijst (ETH Zürich, Switzerland) for valuable discussions and suggestions during the preparation of this manuscript, and Professor A. Dieter Schlüter (ETH Zürich, Switzerland) for his generous support. Funding from Fonds der Chemischen Industrie (Fonds-Stipendium, E. Jahnke), and Schweizerischer Nationalfonds (SNF-Projekt 200021-113509) is gratefully acknowledged.

- [1] a) R. Lakes, *Nature* **1993**, *361*, 511; b) D. Tirrell, *Hierarchical Structures in Biology as a Guide for New Materials Technology*, Technology Report, Washington, **1994**; c) M. Muthukumar, C. K. Ober, E. L. Thomas, *Science* **1997**, *277*, 1225; d) S. Hecht, *Mater. Today* **2005**, *8*, 48; e) C. J. Hawker, K. L. Wooley, *Science* **2005**, *309*, 1200; f) E. W. Meijer, A. P. H. J. Schenning, *Nature* **2002**, *419*, 353.  
 [2] F. J. M. Hoeben, P. Jonkheijm, E. W. Meijer, A. P. H. J. Schenning, *Chem. Rev.* **2005**, *105*, 1491.  
 [3] a) S. H. Gellman, *Acc. Chem. Res.* **1998**, *31*, 173; b) D. J. Hill, M. J. Mio, R. B. Prince, T. S. Hughes, J. S. Moore, *Chem. Rev.* **2001**, *101*,

3893; c) *Foldamers—Structure, Properties, and Applications* (Eds.: S. Hecht, I. Huc), Wiley-VCH, Weinheim (Germany), **2007**.

- [4] a) J. J. L. M. Cornelissen, J. J. M. Donners, R. de Gelder, W. S. Graswinckel, G. A. Metselaar, A. E. Rowan, N. A. J. M. Sommerdijk, R. J. M. Nolte, *Science* **2001**, *293*, 676; b) J. J. L. M. Cornelissen, M. Fischer, N. A. J. M. Sommerdijk, R. J. M. Nolte, *Science* **1998**, *280*, 1427; c) A. Kros, W. Jesse, G. A. Metselaar, J. J. L. M. Cornelissen, *Angew. Chem.* **2005**, *117*, 4423; *Angew. Chem. Int. Ed.* **2005**, *44*, 4349.  
 [5] For selected examples, see a) R. Nomura, J. Tabei, T. Masuda, *J. Am. Chem. Soc.* **2001**, *123*, 8430; b) G. Gao, F. Sanda, T. Masuda, *Macromolecules* **2003**, *36*, 3932; c) G. Gao, F. Sanda, T. Masuda, *Macromolecules* **2003**, *36*, 3938; d) H. Zhao, F. Sanda, T. Masuda, *Macromolecules* **2004**, *37*, 8888; e) J. Tabei, M. Shiotsuki, F. Sanda, T. Masuda, *Macromolecules* **2005**, *38*, 9448.  
 [6] A preorganization of monomers has, for instance, been proposed for certain dendronized monomers (see H. Frauenrath, *Prog. Polym. Sci.* **2005**, *30*, 325) and in the case of the described polymerization of oligopeptide-substituted isocyanides (see ref. [4] as well as, for instance, G. A. Metselaar, J. J. L. M. Cornelissen, A. E. Rowan, R. J. M. Nolte, *Angew. Chem.* **2005**, *117*, 2026; *Angew. Chem. Int. Ed.* **2005**, *44*, 1990).  
 [7] a) A. Mueller, D. F. O'Brien, *Chem. Rev.* **2002**, *102*, 727; b) H. Ringsdorf, B. Schlarb, J. Venzmer, *Angew. Chem.* **1988**, *100*, 117; *Angew. Chem. Int. Ed. Engl.* **1988**, *27*, 113.  
 [8] G. R. Desiraju, *Angew. Chem.* **1995**, *107*, 2541; *Angew. Chem. Int. Ed. Engl.* **1995**, *34*, 2311; .  
 [9] a) G. Wegner, *Z. Naturforsch. B* **1969**, *24*, 824; b) V. Enkelmann, *Adv. Polym. Sci.* **1984**, *63*, 91.  
 [10] a) B. Tieke, G. Wegner, D. Naegele, H. Ringsdorf, *Angew. Chem.* **1976**, *88*, 805; *Angew. Chem. Int. Ed. Engl.* **1976**, *15*, 764; ; b) D. N. Batchelder, S. D. Evans, T. L. Freeman, L. Häussling, H. Ringsdorf, H. Wolf, *J. Am. Chem. Soc.* **1994**, *116*, 1050; c) D. W. Britt, U. G. Hofmann, D. Möbius, S. W. Hell, *Langmuir* **2001**, *17*, 3757; d) Y. Okawa, M. Aono, *Nature* **2001**, *409*, 683; e) A. Miura, S. De Feyter, M. M. S. Abdel-Mottaleb, A. Gesquiere, P. C. M. Grim, G. Moensner, M. Sieffert, M. Klapper, K. Müllen, F. C. De Schryver, *Langmuir* **2003**, *19*, 6474; f) S. P. Sullivan, A. Schnieders, S. K. Mbugua, T. P. Beebe, *Langmuir* **2005**, *21*, 1322; g) J. Y. Chang, J. H. Baik, C. B. Lee, M. J. Han, S.-K. Hong, *J. Am. Chem. Soc.* **1997**, *119*, 3197; h) J. Y. Chang, J. R. Yeon, Y. S. Shin, M. J. Han, S.-K. Hong, *Chem. Mater.* **2000**, *12*, 1076; i) S. J. Lee, C. R. Park, J. Y. Chang, *Langmuir* **2004**, *20*, 9513; j) S. Okada, S. Peng, W. Spevak, D. Charych, *Acc. Chem. Res.* **1998**, *31*, 229; k) S. Svenson, P. B. Messersmith, *Langmuir* **1999**, *15*, 4464; l) Q. Cheng, M. Yamamoto, R. C. Stevens, *Langmuir* **2000**, *16*, 5333; m) S. B. Lee, R. Koepsel, D. B. Stolz, H. E. Warriner, A. J. Russell, *J. Am. Chem. Soc.* **2004**, *126*, 13400; n) M. Masuda, T. Hanada, Y. Okada, K. Yase, T. Shimizu, *Macromolecules* **2000**, *33*, 9233; o) M. George, R. G. Weiss, *Chem. Mater.* **2003**, *15*, 2879; p) Z. Yuan, C.-W. Lee, S.-H. Lee, *Angew. Chem.* **2004**, *116*, 4293; *Angew. Chem. Int. Ed.* **2004**, *43*, 4197; ; q) O. J. Dautel, M. Robitzer, J. P. Lere-Porte, F. Serein-Spirau, J. J. E. Moreau, *J. Am. Chem. Soc.* **2006**, *128*, 16213.

- [11] L. Brunsveld, B. J. B. Folmer, E. W. Meijer, R. P. Sijbesma, *Chem. Rev.* **2001**, *101*, 4071.
- [12] a) D. J. Selkoe, *Nature* **2003**, *426*, 900; b) R. Tycko, *Curr. Opin. Struct. Biol.* **2004**, *14*, 96; c) O. S. Makin, L. C. Serpell, *FEBS J.* **2005**, *272*, 5950; d) R. Nelson, D. Eisenberg, *Adv. Protein Chem.* **2006**, *73*, 235.
- [13] a) M. Sunde, L. C. Serpell, M. Bartlam, P. E. Fraser, M. B. Pepys, C. C. F. Blake, *J. Mol. Biol.* **1997**, *273*, 729; b) O. Sumner Makin, L. C. Serpell, *J. Mol. Biol.* **2004**, *335*, 1279.
- [14] a) O. N. Antzutkin, J. J. Balbach, R. D. Leapman, N. W. Rizzo, J. Reed, R. Tycko, *Proc. Natl. Acad. Sci. USA* **2000**, *97*, 13045; b) A. T. Petkova, Y. Ishii, J. J. Balbach, O. N. Antzutkin, R. D. Leapman, F. Delaglio, R. Tycko, *Proc. Natl. Acad. Sci. USA* **2002**, *99*, 16742; c) T. Luhrs, C. Ritter, M. Adrian, D. Riek-Loher, B. Bohrmann, H. Döbeli, D. Schubert, R. Riek, *Proc. Natl. Acad. Sci. USA* **2005**, *102*, 17342; d) F. Shewmaker, R. B. Wickner, R. Tycko, *Proc. Natl. Acad. Sci. USA* **2006**, *103*, 19754; e) J. C. C. Chan, N. A. Oyler, W.-M. Yau, R. Tycko, *Biochemistry* **2005**, *44*, 10669; f) A. V. Kajava, U. Baxa, R. B. Wickner, A. C. Steven, *Proc. Natl. Acad. Sci. USA* **2004**, *101*, 7885; g) A. V. Kajava, U. Aebi, A. C. Steven, *J. Mol. Biol.* **2005**, *348*, 247; h) J. L. Jimenez, E. J. Nettleton, M. Bouchard, C. V. Robinson, C. M. Dobson, H. R. Saibil, *Proc. Natl. Acad. Sci. USA* **2002**, *99*, 9196.
- [15] In a parallel, in-register  $\beta$ -sheet, adjacent oligopeptide  $\beta$ -strands are arranged parallel to one another with the same directionality and without a lateral displacement.
- [16] These serpentine structures of  $\beta$ -strands have, somewhat misleadingly, been termed “superpleated  $\beta$ -sheets” (ref. [12]); the term “superpleated  $\beta$ -strands” may appear to be more appropriate.
- [17] a) J. Jenkins, R. Pickersgill, *Prog. Biophys. Mol. Biol.* **2001**, *77*, 111; b) M. F. Perutz, J. T. Finch, J. Berriman, A. Lesk, *Proc. Natl. Acad. Sci. USA* **2002**, *99*, 5591; c) H. Wille, M. D. Michelitsch, V. Guenebaut, S. Supattapone, A. Serban, F. E. Cohen, D. A. Agard, S. B. Prusiner, *Proc. Natl. Acad. Sci. USA* **2002**, *99*, 3563.
- [18] a) R. Nelson, M. R. Sawaya, M. Balbirnie, A. O. Madsen, C. Riekel, R. Grothe, D. Eisenberg, *Nature* **2005**, *435*, 773; b) M. R. Sawaya, S. Sambashivan, R. Nelson, M. I. Ivanova, S. A. Sievers, M. I. Apostol, M. J. Thompson, M. Balbirnie, J. J. W. Wiltzius, H. T. McFarlane, A. O. Madsen, C. Riekel, D. Eisenberg, *Nature* **2007**, *447*, 453.
- [19] In the case of Ure2p, for example, the protein retains its native activity even after fibrillization. It has been proposed that the protofilament spines are just formed from a small segment, that the major part of the protein remains in its native conformation, and that it “dangles at the edges” of the filaments.
- [20] a) A. Aggeli, M. Bell, N. Boden, J. N. Keen, P. F. Knowles, T. C. McLeish, M. Pitkeathly, S. E. Radford, *Nature* **1997**, *386*, 259; b) A. Aggeli, I. A. Nyrkova, M. Bell, R. Harding, L. Carrick, T. C. B. McLeish, A. N. Semenov, N. Boden, *Proc. Natl. Acad. Sci. USA* **2001**, *98*, 11857; c) C. W. G. Fishwick, A. J. Beevers, L. M. Carrick, C. D. Whitehouse, A. Aggeli, N. Boden, *NanoLett.* **2003**, *3*, 1475; d) C. Whitehouse, J. Fang, A. Aggeli, M. Bell, R. Brydson, C. W. G. Fishwick, J. R. Henderson, C. M. Knobler, R. W. Owens, N. H. Thomson, D. A. Smith, N. Boden, *Angew. Chem.* **2005**, *117*, 2001; *Angew. Chem. Int. Ed.* **2005**, *44*, 1965.
- [21] If the tapes’ surfaces are equivalent, there is neither a driving force for curling up nor for selective dimerization, that is, ribbon formation. Instead, the tapes will rather be twisted instead, and directly form fibrils with  $n$  stacked  $\beta$ -sheet tapes.
- [22] Boden and co-workers had designed their synthetic oligopeptide systems specifically aiming at antiparallel  $\beta$ -sheet formation and, accordingly, limited the scope of their model. Of course, the assumed antiparallel  $\beta$ -sheet formation implicitly excluded any residual dipole moment component in the  $\beta$ -sheet plane perpendicular to the tapes’ axes. Conversely, the assumption of amphiphilic  $\beta$ -sheets implicitly included the presence of dipole moment components perpendicular to the  $\beta$ -sheet plane. Nevertheless, one has to be aware that, for example, the formation of  $\beta$ -sheets with parallel  $\beta$ -strand orientation should result in a non-zero dipole moment component in the  $\beta$ -sheet plane perpendicular to the tape axis (see W. G. J. Hol, L. M. Halie, C. Sander, *Nature* **1981**, *294*, 532). Likewise, the presence of an uneven number of N-H $\cdots$ O=C backbone hydrogen bonding sites should result in a residual dipole moment component in tape direction (see, for example, S. Krauthäuser, L. A. Christianson, D. R. Powell, S. H. Gellman, *J. Am. Chem. Soc.* **1997**, *119*, 11719). While the latter can straightforwardly be compensated on the ribbon level, it would constitute a non-negligible additional energetic contribution to ribbon formation even in the case of non-amphiphilic  $\beta$ -sheet tapes.
- [23] a) T. S. Burkoth, T. L. S. Benzinger, D. N. M. Jones, K. Hallenga, S. C. Meredith, D. G. Lynn, *J. Am. Chem. Soc.* **1998**, *120*, 7655; b) T. S. Burkoth, T. L. S. Benzinger, V. Urban, D. G. Lynn, S. C. Meredith, P. Thiyagarajan, *J. Am. Chem. Soc.* **1999**, *121*, 7429; c) T. S. Burkoth, T. L. S. Benzinger, V. Urban, D. M. Morgan, D. M. Gregory, P. Thiyagarajan, R. E. Botto, S. C. Meredith, D. G. Lynn, *J. Am. Chem. Soc.* **2000**, *122*, 7883; d) J. Hentschel, E. Krause, H. G. Börner, *J. Am. Chem. Soc.* **2006**, *128*, 7722; e) H. Rettig, E. Krause, H. G. Börner, *Macromol. Rapid Commun.* **2004**, *25*, 1251; f) J. Hentschel, H. G. Börner, *J. Am. Chem. Soc.* **2006**, *128*, 14142.
- [24] H. A. Lashuel, S. R. LaBrenz, L. Woo, L. C. Serpell, J. W. Kelly, *J. Am. Chem. Soc.* **2000**, *122*, 5262.
- [25] This molecular architecture was chosen because, typically, five or more (ValThr) repeats are necessary to obtain stable  $\beta$ -sheets from linear precursors in aqueous solution. The preorganization of the short oligopeptide segments with an appropriate rigid spacer induces an enhanced aggregation behavior. Compare a) C. L. Nesloney, J. W. Kelly, *Bioorg. Med. Chem.* **1996**, *4*, 739; b) K. Janek, J. Behlke, J. Zipper, H. Fabian, Y. Georgalis, M. Beyer mann, M. Bienert, E. Krause, *Biochemistry* **1999**, *38*, 8246.
- [26] While the selective formation of ribbons in protic environments would involve interactions between the more hydrophobic surfaces, it may be mediated by, for instance, hydrogen bonding between the more hydrophilic surfaces in apolar solvents.
- [27] a) E. Jahnke, I. Lieberwirth, N. Severin, J. P. Rabe, H. Frauenrath, *Angew. Chem.* **2006**, *118*, 5510; *Angew. Chem. Int. Ed.* **2006**, *45*, 5383; ; b) E. Jahnke, A.-S. Millerioux, N. Severin, J. P. Rabe, H. Frauenrath, *Macromol. Biosci.* **2007**, *7*, 136; c) E. Jahnke, A.-S. Millerioux, N. Severin, J. P. Rabe, H. Frauenrath, *Adv. Mater.* **2008**, *20*, 409–414.
- [28] Any detailed conclusions from IR spectra are complicated by the fact that the assignments of IR bands to protein secondary structures in the literature are contradictory. For good reviews of this issue, see B. R. Singh in *Infrared Analysis of Peptides and Proteins* (Ed.: B. R. Singh), *ACS Symposium Series 750*, **2000**, 2–37; S. Krimm, in *Infrared Analysis of Peptides and Proteins* (Ed.: B. R. Singh), *ACS Symposium Series 750*, **2000**, 38–53; P. I. Haris, in *Infrared Analysis of Peptides and Proteins* (Ed.: B. R. Singh), *ACS Symposium Series 750*, **2000**, 54–95. Furthermore, the aggregation in organic media in the present work will lead to different results as compared to IR spectra performed in protic environments.

Published online: January 28, 2008